Int. J. Heat Mass Transfer. Vol. 28, No. 5, pp. 995–1003, 1985
Printed in Great Britain

0017–9310/85 $3.00 + 0.00

Effect of buoyancy on laminar fully developed flow in a vertical annular passage with radial internal fins

C. PRAKASH* and P. RENZONI
Department of Mechanical Engineering, Aeronautical Engineering and Mechanics, Rensselaer Polytechnic Institute, Troy, NY 12181, U.S.A.

(*Received* 7 *June* 1984 *and in final form* 2 *November* 1984)

Abstract—Laminar fully developed flow in an internally finned vertical concentric circular annular duct has been numerically analysed. The fins are radial and affixed on the outside of the inner tube. The outer wall is insulated, while a uniform heat input is applied at the inner tube (buoyancy aiding the flow). It is found that buoyancy increases both the friction and the heat transfer. The effect, compared relative to the no buoyancy case, is stronger when the number of fins is small or the fins are short. Accounting for the buoyancy effects, a finned passage appears to be an even more effective heat exchange device.

INTRODUCTION

THE CONCENTRIC circular annular duct is an important geometry for many fluid flow and heat transfer devices. Indeed, the simplest form of a two-fluid heat exchanger is a double pipe made up of two concentric circular tubes. The analysis of flow and heat transfer in this geometry is therefore very important from an engineering standpoint.

For the purpose of heat transfer augmentation, fins are often employed in heat exchange devices [1, 2]. In a double pipe heat exchanger, the fins may be employed on the inside of the inner tube or in the annular region. The finned annular passage has been the subject of some earlier studies [3–6], but the effect of buoyancy on flow and heat transfer has not been examined before. Such an effect can be quite important, and it is this recognition that constitutes the motivation for the present work.

ANALYSIS

The problem statement

The problem to be investigated concerns laminar fully developed combined free and forced convection flow in a vertical internally finned concentric circular annular duct. The flow is against gravity, i.e. in the vertical direction. The fins are radial, assumed to be of zero thickness, and affixed on the outside of the inner tube. The cross-section of the duct is shown in Fig. 1; a, b and h represent the inner tube radius, the outer tube radius and the fin height respectively. A uniform heat input Q per unit axial length is applied to the inner tube, while the outer tube is taken to be insulated.

Assumptions

The fins are assumed to be made of a highly conducting material (100% efficient). Hence, at any cross-section, the inner tube and the fins have a uniform temperature. All fluid properties are assumed constant except for the variation of density in the buoyancy term which is computed using the Boussinesq approximation. Finally, viscous dissipation and compression work terms are neglected in the energy equation.

Governing equations

For fully developed flow, the velocity components in the cross-sectional plane are zero and the axial velocity w is itself independent of the axial distance z. Further, for the thermal boundary conditions considered, all temperatures rise linearly in the axial direction at the same rate. The equations governing the problem are:

$$\mu\left[\frac{1}{r}\frac{\partial}{\partial r}\left(r\frac{\partial w}{\partial r}\right)+\frac{1}{r^2}\frac{\partial^2 w}{\partial \theta^2}\right]=\frac{\mathrm{d}p}{\mathrm{d}z}+\rho g \qquad (1)$$

$$\alpha\left[\frac{1}{r}\frac{\partial}{\partial r}\left(r\frac{\partial T}{\partial r}\right)+\frac{1}{r^2}\frac{\partial^2 T}{\partial \theta^2}\right]=w\frac{\partial T}{\partial z} \qquad (2)$$

where T represents the temperature and $\mathrm{d}p/\mathrm{d}z$ is the uniform pressure gradient in the axial direction. Other symbols have their usual meaning and are described in the nomenclature.

Let $T_w(z)$ be the uniform temperature of the inner tube and the fins at an axial location z. With the Boussinesq approximation, the density ρ at this cross-section can be represented as

$$\rho=\rho_w[1+\beta(T_w-T)] \qquad (3)$$

where β is the coefficient of volumetric expansion and ρ_w, is the density corresponding to T_w. Since T_w rises linearly with z, ρ_w is a function of z. However, in accordance with the constant-density approximation, we replace ρ_w by a constant density ρ_0 corresponding to some reference location. Thus,

$$\rho=\rho_0[1+\beta(T_w-T)]. \qquad (4)$$

* Present address: CHAM of North America, Inc., 1525-A Sparkman Drive, Huntsville, AL 35805, U.S.A.

NOMENCLATURE

a	inner tube radius
b	outer tube radius
c	specific heat of the fluid
f	friction factor, equation (18)
fRe	product of the friction factor f and the Reynolds number Re, equation (19)
$(fRe)_0$	fRe corresponding to the zero Rayleigh number (no buoyancy) case
Gr	Grashof number, equation (16)
g	acceleration due to gravity
h	fin height
h_T	heat transfer coefficient, equation (22)
k	thermal conductivity of the fluid
$\dot{m}$	mass flow rate through the duct
N	number of fins
Nu	Nusselt number, equation (23)
Nu_0	Nu corresponding to the zero Rayleigh number (no buoyancy) case
p	pressure
Q	total heat input per unit axial length
R	dimensionless radial coordinate, equation (8)
Ra	Rayleigh number, equation (15)
Re	Reynolds number, equation (17)
r	radial coordinate
T	temperature
T_w	inner tube and fin temperature
T_b	bulk temperature, equation (6)
w	axial velocity
$\bar{w}$	average axial velocity
z	axial coordinate.

Greek symbols

α	thermal diffusivity of the fluid, $k/\rho_0 c$
β	coefficient of thermal expansion
Θ	dimensionless temperature, equation (10)
θ	angular coordinate
μ	viscosity
ν	kinematic viscosity, μ/ρ_0
ρ	density
ρ_w	density corresponding to wall temperature T_w
ρ_0	reference constant density
Ω	dimensionless axial velocity, equation (9).

The axial temperature gradient $(\partial T/\partial z)$ can be related to the heat input Q per unit axial length by an overall mass balance:

$$\frac{\partial T}{\partial z} = \frac{dT_w}{dz} = \frac{dT_b}{dz} = \frac{Q}{\dot{m}c} \tag{5}$$

where T_b is the bulk temperature defined by

$$T_b = \int\int wTr\,dr\,d\theta \Big/ \int\int wr\,dr\,d\theta \tag{6}$$

and $\dot{m}$ is the mass flow rate given by

$$\dot{m} = \rho_0 \bar{w}\pi(b^2 - a^2) = \rho_0 \int\int wr\,dr\,d\theta. \tag{7}$$

In equations (6) and (7) the integration is over the cross-section of the annular region, and equation (7) defines the average velocity $\bar{w}$.

The problem can be nondimensionalized by introducing

$$R = r/a \tag{8}$$

$$\Omega = w\mu \Big/ \left[a^2\left(-\frac{dp}{dz} - \rho_0 g\right)\right] \tag{9}$$

and

$$\Theta = (T - T_w)/(Q/k) \tag{10}$$

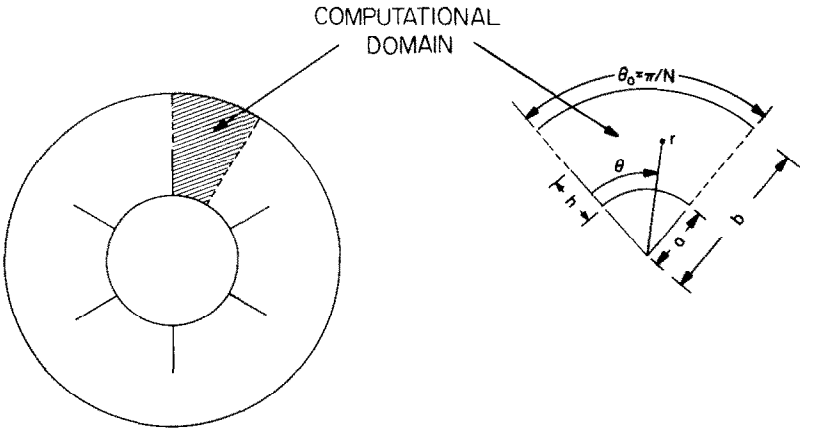

FIG. 1. Internally finned annular passage.

where k is the thermal conductivity of the fluid. These definitions lead to the following dimensionless form of the governing equations:

$$\frac{1}{R}\frac{\partial}{\partial R}\left(R\frac{\partial \Omega}{\partial R}\right)+\frac{1}{R^2}\frac{\partial^2 \Omega}{\partial \theta^2}+\left[\pi\frac{(b^2-a^2)}{a^2}\right]Ra\,\bar{\Omega}\Theta+1=0 \quad (11)$$

and

$$\frac{1}{R}\frac{\partial}{\partial R}\left(R\frac{\partial \Theta}{\partial R}\right)+\frac{1}{R^2}\frac{\partial^2 \Theta}{\partial \theta^2}-\left[\frac{a^2}{\pi(b^2-a^2)}\right]\frac{\Omega}{\bar{\Omega}}=0 \quad (12)$$

in which $\bar{\Omega}$ is the mean value of Ω and is related to $\bar{w}$ by

$$\bar{\Omega}=\bar{w}\mu\Big/\left[a^2\left(-\frac{\mathrm{d}p}{\mathrm{d}z}-\rho_0 g\right)\right]. \quad (13)$$

$\bar{\Omega}$ can be calculated from

$$\bar{\Omega}=\int\int \Omega R\,\mathrm{d}R\,\mathrm{d}\theta\Big/\int\int R\,\mathrm{d}R\,\mathrm{d}\theta. \quad (14)$$

The Rayleigh number

In equation (11), Ra represents the Rayleigh number which is the most important parameter of the problem. It is given as

$$Ra=\frac{a^2}{\pi(b^2-a^2)}\frac{Gr}{Re} \quad (15)$$

where Gr and Re are the Grashof and Reynolds numbers defined by

$$Gr=2\rho_0^2\beta g(Q/k)a^3/\mu^2 \quad (16)$$

and

$$Re=\rho_0\bar{w}2a/\mu. \quad (17)$$

The Grashof and Reynolds numbers measure the strengths of free and forced convection respectively. The Rayleigh number is, therefore, a measure of the relative strengths of free and forced convection.

The critical Rayleigh number

The effect of buoyancy is to increase the velocity (aid the flow) near the heated inner tube and the fins. For a fixed mass flow rate, this implies that the velocity near the outer tube must decrease. Beyond a certain critical value of the Rayleigh number, the velocity near the outer wall becomes less than zero, i.e. the flow reverses. Since fully developed solutions involving reverse flows are not expected to occur in practical situations, the numerical computations were not carried out beyond the critical Rayleigh number.

Dimensionless parameters

Besides the Rayleigh number, the problem has three other geometrical parameters; the number of fins N, the radius ratio b/a between the outer and the inner tube, and the dimensionless fin height h/a. A more practical dimensionless fin height definition would be $h/(b-a)$ which ranges from 0 to 1. The following cases were solved for:

$$N=8,16,24$$

$$b/a=1.25,2,5$$

and

$$h/(b-a)=0,0.5,1.$$

For each case, the value of Ra was varied from zero to the critical value.

Boundary conditions

For an arrangement of N equally spaced fins, the required calculation domain is shown in Fig. 1. It is a sector of angle π/N extending from one fin to a location half-way towards the next fin. The boundary conditions for this domain are straightforward: on the inner tube wall and the fin surface, the velocity Ω and the dimensionless temperature Θ are both zero. At the outer tube wall, $\Omega=\partial\Theta/\partial R=0$. The remaining boundaries of the domain, shown by dashed lines, are lines of symmetry implying $\partial\Omega/\partial\theta=\partial\Theta/\partial\theta=0$ there.

Heat transfer and pressure drop parameters

From an engineering standpoint, the important quantities are the friction factor and the Nusselt number. The friction factor f is defined as

$$f=2a(-\mathrm{d}p/\mathrm{d}z-\rho_0 g)/(\rho_0\bar{w}^2/2) \quad (18)$$

and it can easily be shown that

$$fRe=8/\bar{\Omega}. \quad (19)$$

Thus, after a solution for Ω has been obtained, fRe can be obtained from $\bar{\Omega}$.

Consider the temperature difference

$$T_w-T_b=-\bar{\Theta}Q/k \quad (20)$$

where

$$\bar{\Theta}=\int\int \Omega\Theta R\,\mathrm{d}R\,\mathrm{d}\theta\Big/\int\int \Omega R\,\mathrm{d}R\,\mathrm{d}\theta \quad (21)$$

the integration being over the duct cross-section. With external heating applied to the inner tube, the heat transfer coefficient h_T is defined as

$$h_T=\frac{Q}{2\pi a(T_w-T_b)} \quad (22)$$

and thus the Nusselt number Nu is given by

$$Nu=\frac{h_T(2a)}{k}=-\frac{1}{\pi\bar{\Theta}}. \quad (23)$$

COMPUTATIONAL PROCEDURE

In an earlier paper, Prakash and Patankar [7] have considered this very same problem but for an internally finned circular duct. The same numerical procedure has been used here and hence the details will not be repeated. To summarize the salient features, the task here is to solve the coupled Poisson equations (11) and (12) for Ω and Θ. Any numerical formulation can be used to discretize the equations, and the one used here is

the control-volume-based finite-difference method described in [8]. If equations (11) and (12) are solved iteratively one at a time, severe convergence-related difficulties arise as the Rayleigh number increases. To avoid this, the two equations have to be solved in some coupled fashion. This coupling is achieved by solving the discretized forms of equations (11) and (12) using a coupled tri-diagonal matrix algorithm along the different grid lines. Details of this coupled TDMA are available in [7]; a minor difference arises, due to difference in the boundary condition for Ω and Θ at the outer tube, which can easily be worked out. As in [7], a block-correction procedure was used to promote convergence.

The computations were performed on a 22×16 (radial $\times$ angular) grid. A nonuniform grid spacing was used; the grid lines were packed closely near the fin, the fin tip and the inner and outer tube walls. The accuracy of the results using this grid was determined by comparing the results with those available in literature for purely forced convection. The results for fRe and the Nu in the finless annuli are in agreement with those given in [9] and [10] to within 1 and 0.5% respectively. For the finned annuli, where the fins extend from inner tube to the outer tube, the results of fRe are in agreement with those given in [3] to within 1%.

RESULTS

Velocity and temperature profiles

Figure 2 shows the effect of natural convection on the flow velocity for a typical case. Here $w/\bar{w}$ is plotted as a function of the radial coordinate at $\theta = \theta_0$ which corresponds to the symmetry line between two adjacent fins. As expected, the effect of increasing Rayleigh number (i.e. increasing buoyancy effects) is to increase the velocity near the hot inner tube and the fins. For a fixed $\bar{w}$, the velocity near the colder outer wall must decrease. The velocity profile becomes steeper near the walls as the Rayleigh number increases which, as we shall see, is the reason for the friction factor to increase with increasing Rayleigh number.

Temperature profiles for the same location and conditions are shown in Fig. 3. The temperature decreases, as expected, as one moves away from the heated wall. The overall effect of buoyancy is to make the temperature distribution more uniform, i.e. reduce the wall to bulk temperature difference. This, as we shall see, is manifested in the increase of Nusselt number with the Rayleigh number.

Friction and heat transfer

Because of the widely different scales involved, it is convenient to present the results for the friction factor fRe and the Nusselt number Nu with reference to their values for zero Rayleigh number. These reference values are first presented in Table 1. The subscript 0 identifies the case of zero Rayleigh number. The results for non-zero Rayleigh number are normalized with these basic values.

The effect of buoyancy on the friction factor is shown in Figs. 4(a)–(c). For each case, the Rayleigh number range is limited by the critical Rayleigh number. As can be concluded from the figures, the friction factor

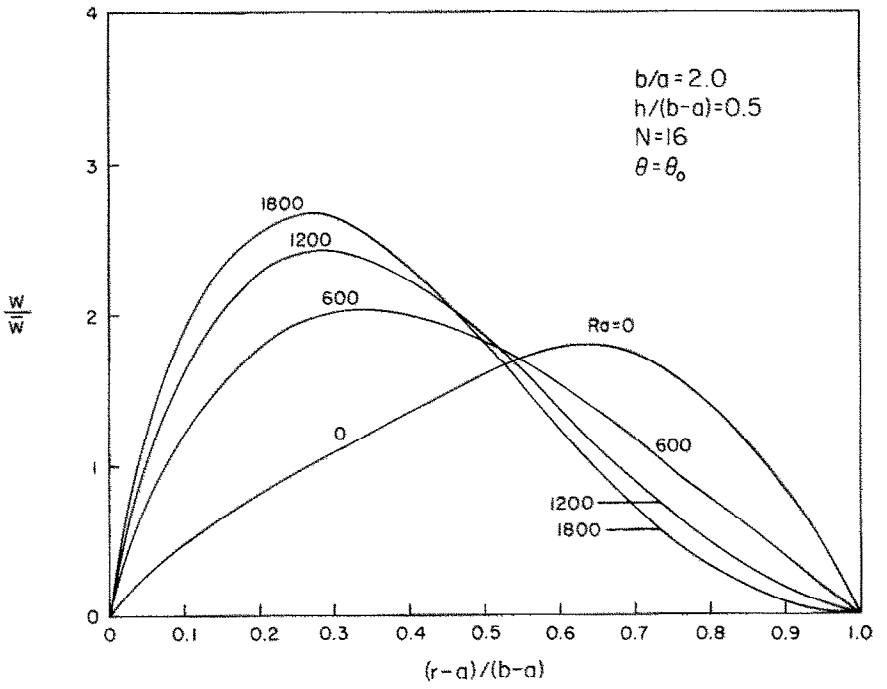

FIG. 2. Effect of buoyancy on the velocity distribution.

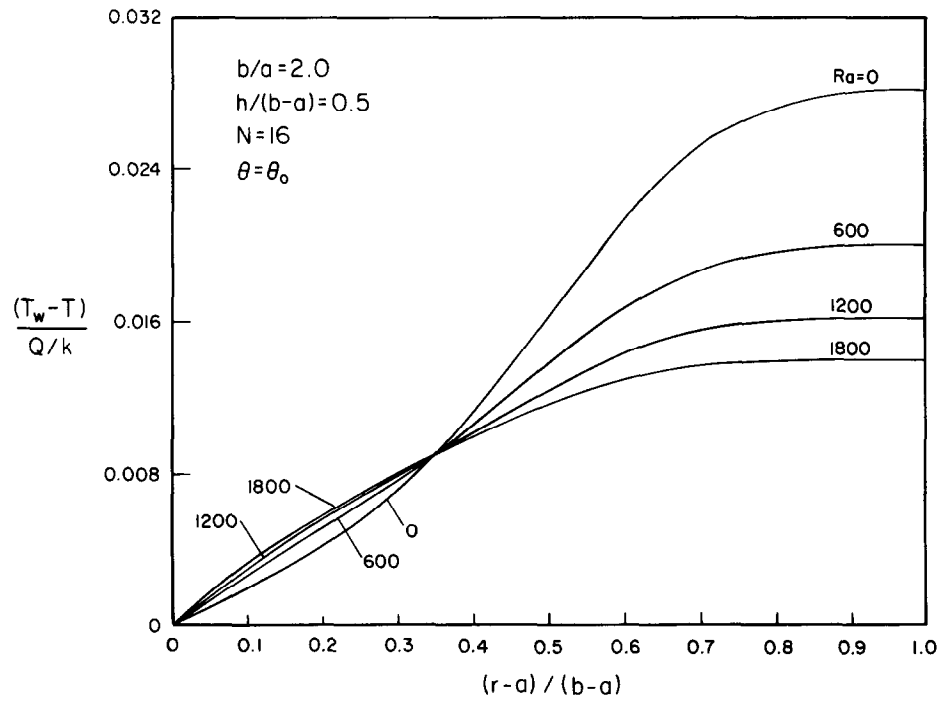

FIG. 3. Effect of buoyancy on the temperature distribution.

increases with the Rayleigh number which, as discussed before, is due to the steeper velocity profile near the fins and the base tube. Measured in terms of the ratio $(fRe)/(fRe)_0$, the effect of buoyancy decreases as the number of fins or the fin height increases. For a fixed Rayleigh number, we have the inequality

$$\frac{(fRe)_{\text{finned}}}{(fRe)_{\text{finless}}} < \frac{(fRe)_{0,\text{finned}}}{(fRe)_{0,\text{finless}}}$$

with the difference increasing as the number of fins or

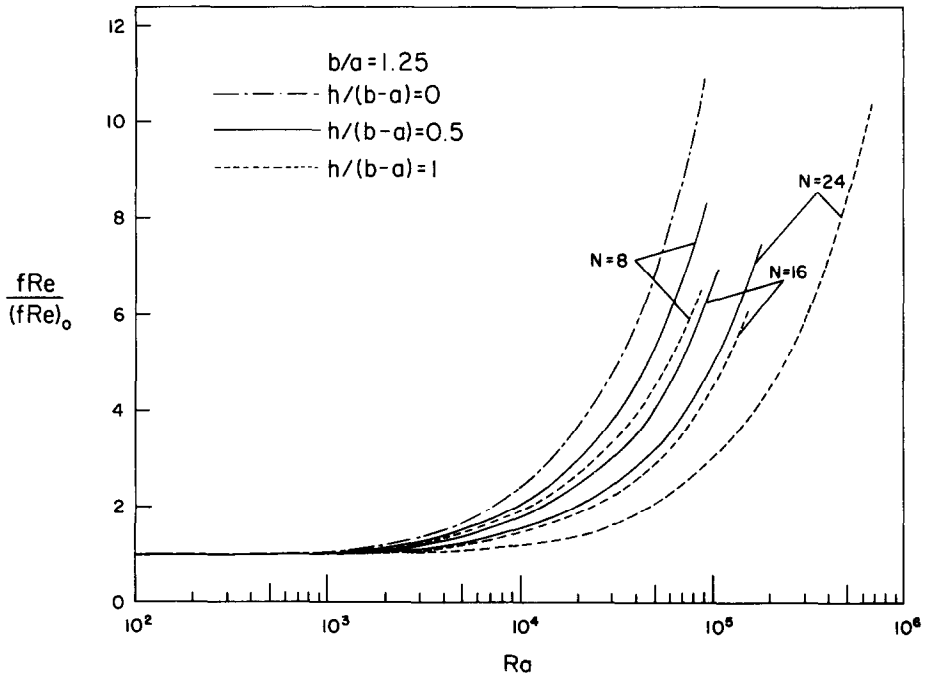

FIG. 4(a). Effect of buoyancy on the friction factor; $b/a = 1.25$.

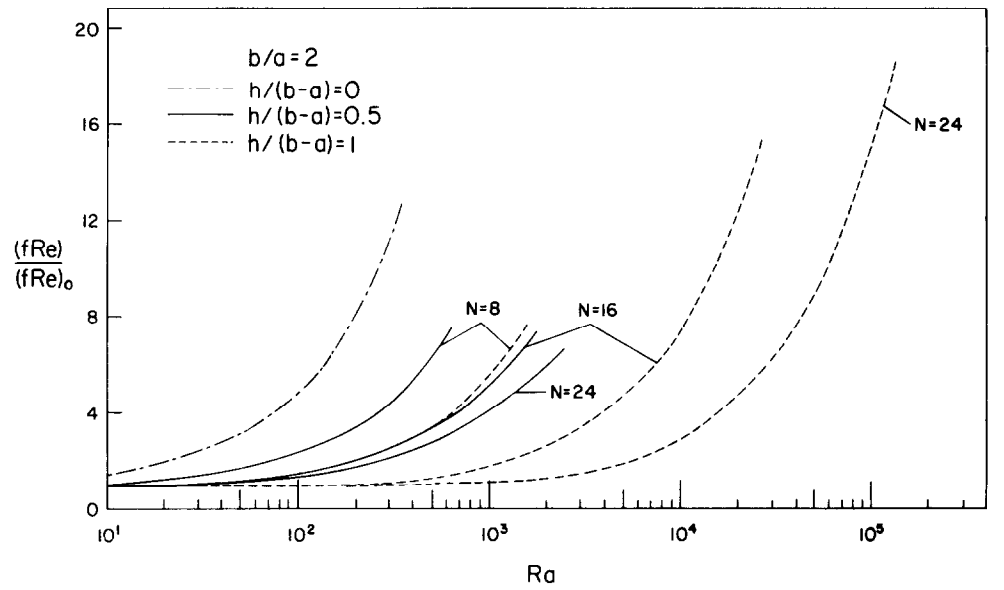

FIG. 4(b). Effect of buoyancy on the friction factor; $b/a = 2$.

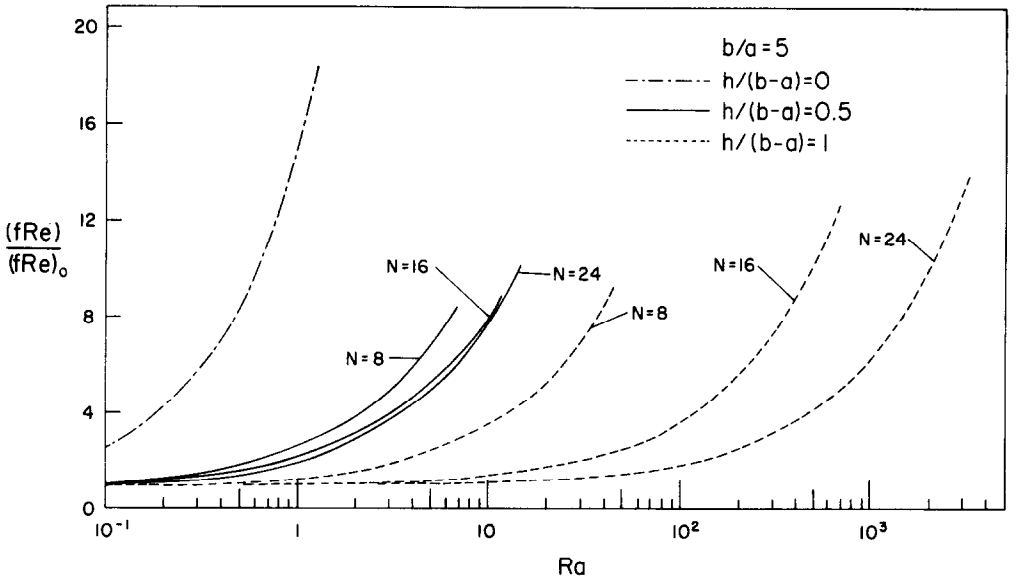

FIG. 4(c). Effect of buoyancy on the friction factor; $b/a = 5$.

Table 1. Baseline results for the zero Rayleigh number (no buoyancy) case

		$(fRe)_0$ $h/(b-a)$				Nu_0 $h/(b-a)$	
	N	0	0.5	1	N	0	0.5	1
$b/a = 1.25$	0	1523.1			0	22.27		
	8		1736.8	1852.4	8		25.37	27.94
	16		2043.1	2359.3	16		31.62	44.33
	24		2430.3	3109.6	24		38.99	71.88
$b/a = 2.0$	0	94.53			0	6.116		
	8		154.73	195.34	8		11.89	21.21
	16		241.78	433.60	16		16.63	64.65
	24		315.78	805.68	24		17.42	133.95
$b/a = 5.0$	0	5.727			0	2.116		
	8		15.29	26.80	8		7.376	26.11
	16		21.76	74.14	16		8.010	82.04
	24		24.97	145.24	24		8.078	165.01

the fin height increases. In fact, for some cases, $(fRe)_{\text{finned}}$ can be less than $(fRe)_{\text{finless}}$. Therefore, buoyancy makes a vertically oriented finned duct an even more attractive heat exchange device.

The effect of buoyancy on the Nusselt number is plotted in Figs. 5(a)–(c). As can be seen, the effect of buoyancy is to increase the Nusselt number. Measured in terms of the ratio Nu/Nu_0, the effect of buoyancy decreases as the number of fins or the fin height increases. However, the ratio Nu/Nu_0 is not very large so that at any given Rayleigh number, the Nu increases with the number of fins and the fin height.

Finally, the critical Rayleigh number increases as the number of fins or the fin height increases.

From all the above considerations it may be concluded that a finned passage is an even more

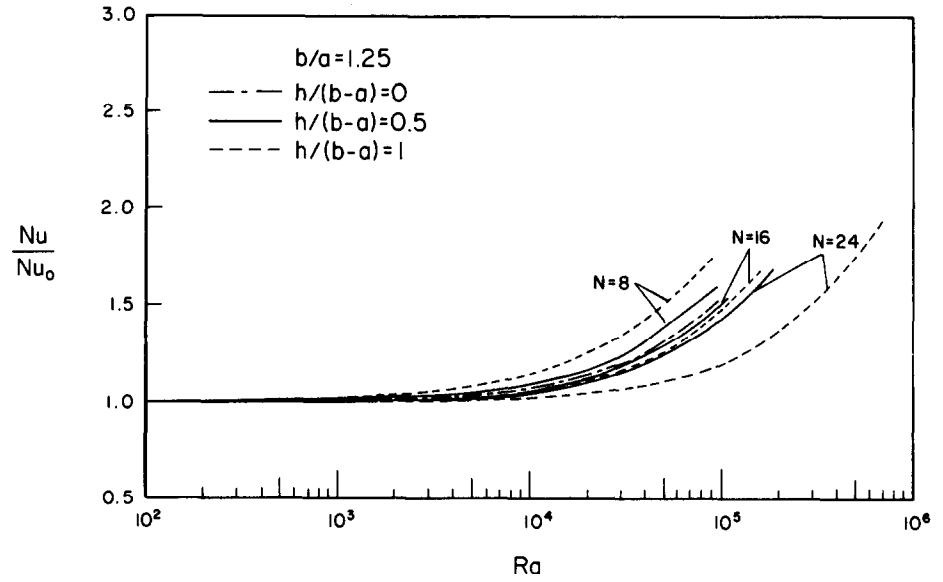

FIG. 5(a). Effect of buoyancy on the Nusselt number; $b/a = 1.25$.

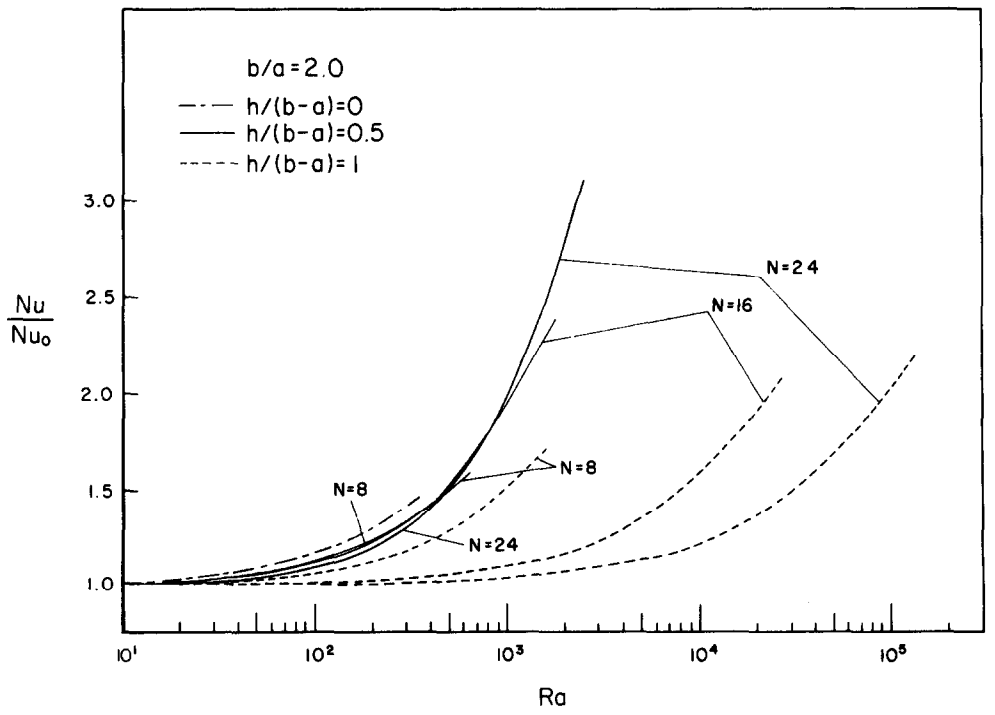

FIG. 5(b). Effect of buoyancy on the Nusselt number; $b/a = 2$.

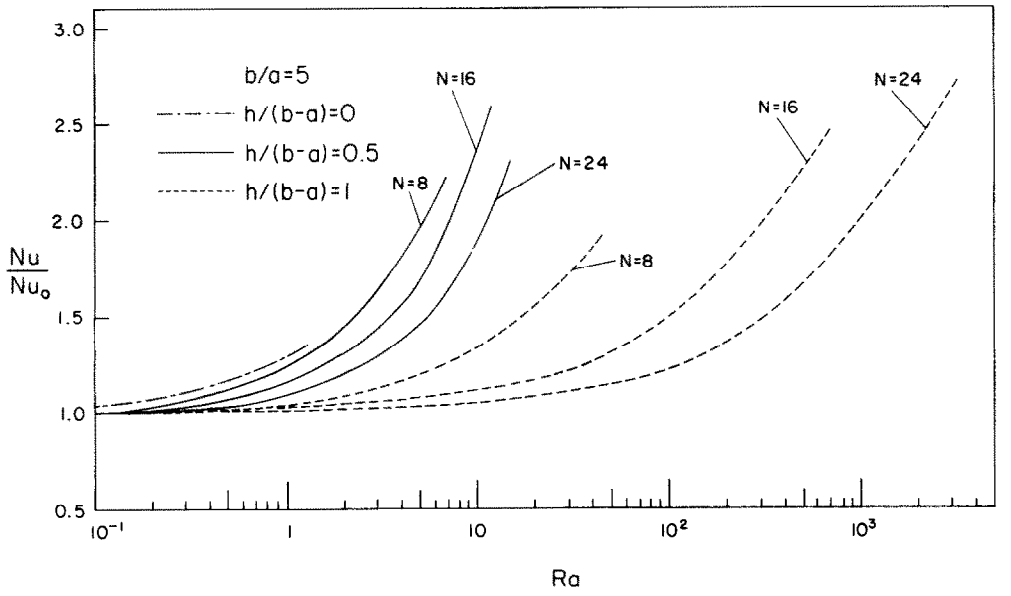

FIG. 5(c). Effect of buoyancy on the Nusselt number; $b/a = 5$.

attractive heat exchange device when the buoyancy effects are accounted for.

CONCLUDING REMARKS

Laminar fully developed combined free and forced convection flow in a vertical internally finned annular passage has been numerically analysed. It is found that buoyancy increases both the friction factor and the heat transfer. It is concluded that a finned passage appears an even more effective heat exchange device when buoyancy effects are accounted for.

Acknowledgement—The authors are grateful to the Department of Mechanical Engineering, Aeronautical Engineering and Mechanics at Rensselaer Polytechnic Institute for supporting this work under the auspicies of this institute's BUILD program.

REFERENCES

1. A. E. Bergles, Survey and evaluation of techniques to augment convective heat and mass transfer. In *Progress in Heat and Mass Transfer*, pp. 331–424. Pergamon Press, New York (1969).
2. R. K. Shah and A. L. London, *Laminar Forced Flow Convection in Ducts*. Academic Press, New York (1978).
3. E. M. Sparrow, T. S. Chen and V. K. Jonsson, Laminar flow and pressure drop in internally finned annular ducts, *Int. J. Heat Mass Transfer* **7**, 583–585 (1964).
4. S. V. Patankar, M. Ivanovic and E. M. Sparrow, Analysis of turbulent flow and heat transfer in internally finned tubes and annuli, *J. Heat Transfer* **101**, 29–37 (1979).
5. B. de Lorenzo and E. D. Anderson, Heat transfer and pressure drop of liquids in double-pipe fin-tube exchangers, *Trans. Am. Soc. Mech. Engrs* **67**, 697–702 (1945).
6. L. Clark and R. E. Winston, Calculation of finside coefficients in longitudinal finned-tube exchangers, *Chem. Engng Prog.* **51**, 147–150 (1955).
7. C. Prakash and S. V. Patankar, Combined free and forced convection in vertical tubes with radial internal fins, *J. Heat Transfer* **103**, 566–572 (1981).
8. S. V. Patankar, *Numerical Heat Transfer and Fluid Flow*. Hemisphere Publishing, Washington (1980).
9. T. S. Lundgen, E. M. Sparrow and J. B. Starr, Pressure drop due to the entrance region in ducts of arbitrary cross-section, *J. Basic Engng* **86**, 620–626 (1964).
10. R. E. Lundberg, P. A. McCuen and W. C. Reynolds, Heat transfer in annular passages: hydrodynamically developed laminar flow with arbitrarily prescribed wall temperatures or heat fluxes, *Int. J. Heat Mass Transfer* **6**, 495–529 (1963).

EFFET DE PESANTEUR SUR UN ECOULEMENT LAMINAIRE ETABLI DANS UN PASSAGE ANNULAIRE VERTICAL MUNI D'AILETTES INTERNES RADIALES

Résumé—On analyse numériquement l'écoulement laminaire établi dans un conduit annulaire concentrique, vertical, avec des ailettes internes. Les ailettes sont radiales et fixées sur l'extérieur du tube intérieur. La paroi externe est isolée tandis qu'un flux uniforme est appliqué sur le tube intérieur (la pesanteur aidant l'écoulement). La pesanteur augmente à la fois le frottement et le transfert thermique. L'effet, en comparaison du cas sans pesanteur, est plus fort quand le nombre d'ailettes est faible ou que les ailettes sont courtes. En tenant compte des effets de pesanteur, un passage aileté semble être une conception d'échangeur de chaleur plus efficace.

DER EINFLUSS DES AUFTRIEBS AUF DIE VOLL AUSGEBILDETE LAMINARE STRÖMUNG IN EINEM SENKRECHTEN RINGFÖRMIGEN QUERSCHNITT MIT RADIALEN INNEREN RIPPEN

Zusammenfassung—Die voll ausgebildete laminare Strömung in einem innen berippten kreisringförmigen Kanal wurde numerisch untersucht. Die Rippen sind radial angeordnet und auf der Außenseite des inneren Rohres befestigt. Die äußere Wand ist wärmegedämmt, während eine einheitliche Wärmezufuhr durch das Innenrohr erfolgt (die natürliche Konvektion unterstützt die Strömung). Die Auftriebsströmung erhöht sowohl die Reibung als auch den Wärmeübergang. Dieser Effekt ist stärker, wenn die Anzahl der Rippen klein ist oder die Rippen kurz sind.

ВЛИЯНИЕ ПОДЪЕМНОЙ СИЛЫ НА ЛАМИНАРНОЕ ПОЛНОСТЬЮ РАЗВИТОЕ ТЕЧЕНИЕ В ВЕРТИКАЛЬНОМ КОЛЬЦЕВОМ КАНАЛЕ С РАДИАЛЬНЫМИ ВНУТРЕННИМИ РЕБРАМИ

Аннотация—Численно анализируется ламинарное полностью развитое течение в оребренном изнутри вертикальном концентрическом кольцевом канале. Радиальные ребра прикрепляются к внешней стенке внутренней трубы. Наружная стенка канала изолирована, в то время как однородный тепловой поток подводится к внутренней трубе (подъемная сила способствует течению). Установлено, что подъемная сила увеличивает как трение, так и теплообмен. Это влияние становится более сильным при малых числе и длине ребер по сравнению с отсутствием подъемной силы. При учете воздействия подъемной силы оребренный канал оказывается более эффективным теплообменником.